

Neutron diffraction studies on $\text{Ca}_{1-x}\text{Ba}_x\text{Zr}_4\text{P}_6\text{O}_{24}$ solid solutions

S N ACHARY^{1,*}, O D JAYAKUMAR¹, S J PATWE¹, A B SHINDE²,
P S R KRISHNA², S K KULSHRESHTHA¹ and A K TYAGI¹

¹Chemistry Division; ²Solid State Physics Division, Bhabha Atomic Research Centre,
Mumbai 400 085, India

*Corresponding author

E-mail: sachary@barc.gov.in; aktyagi@barc.gov.in

Abstract. Herein we report the results of detailed crystallographic studies of $\text{Ca}_{1-x}\text{Ba}_x\text{Zr}_4\text{P}_6\text{O}_{24}$ compositions from combined Rietveld refinements of powder X-ray and neutron diffraction data. All the studied compositions crystallize in rhombohedral lattice (space group R-3 No. 148). A continuous solid solution is concluded from the systematic variation of unit cell parameters. The variation of unit cell parameters with the composition indicates decreasing trend in a parameter with increasing Ba^{2+} concentration contrast to an increasing trend in c parameter.

Keywords. Neutron diffraction; X-ray diffraction; Rietveld refinement; crystal structure; NZP ceramics; phosphates.

PACS Nos 61.66.-f; 61.05.F; 61.05.cp; 65.40.Dc

1. Introduction

The materials belonging to NZP ($\text{NaZr}_2\text{P}_3\text{O}_{12}$) class are promising candidates for high temperature structural materials due to their chemical stability, low thermal expansion and low thermal conductivity and fast ionic conductivity [1]. In addition, NZP bears special attention for disposal of nuclear waste materials as a significant extent of diversified chemical elements that can be accommodated in the lattice [2]. The NZP crystallizes in a rhombohedral lattice (space group R-3c) formed by linking ZrO_6 octahedral and PO_4 tetrahedral units [3]. The Na atom occupies the voids of the ZrO_6 and PO_4 frame to balance the excess charge. The general formula for NZP structured materials can be explained as $[M][M'][A]_2[B]_3\text{O}_{12}$, where M and M' (3a and 3b sites of space group R-3c) are Na atoms. However, the M and M' sites can also be replaced by higher charge cations without disturbing the basic frame of NZP lattice.

In general, the thermal expansion behaviours of NZP structured compounds are anisotropic and the nature of anisotropy depends on the size and charge of the M and M' site cations [1]. The magnitude and nature of thermal expansion of

the NZP has been attributed to the weak nature of Na–O bonds. The title compounds $\text{MZr}_4\text{P}_6\text{O}_{24}$ belong to NZP family, where Na is replaced by the divalent (M) cations. The $\text{MZr}_4\text{P}_6\text{O}_{24}$ compounds also exhibit similar chemical and thermal stabilities as well as lower values of overall thermal expansion coefficients [4]. The detailed thermal expansion behaviours of these materials with various divalent cations have been studied extensively. Though, all these materials crystallize in similar rhombohedral lattices, the axial thermal expansion coefficients differ with the nature and ionic radii of M^{2+} cations. For example, in $\text{CaZr}_4\text{P}_6\text{O}_{24}$, the a -axis increases with temperature in contrast to a decreasing trend of the c -axis. However, an opposite trend of axial thermal expansion has been reported for the Ba and Sr analogue compounds [4,5]. The significant anisotropy in the thermal expansion causes an appreciable internal strain among the grains. Thus, these materials show poor sinterability. The mixed alkaline earth metal ion compositions, such as $\text{Ca}_{1-x}\text{Sr}_x\text{Zr}_4\text{P}_6\text{O}_{24}$ and $\text{Ca}_{1-x}\text{Ba}_x\text{Zr}_4\text{P}_6\text{O}_{24}$ are likely to show controlled anisotropic thermal expansion. The lack of crystal structure data for such solid solutions limits this explanation. We need to mention here that the replacement of Na by the divalent cation brings a change in symmetry from R-3c to R-3 [6]. The symmetry change is attributed to the ordering of vacancies in the unit cell. Structural studies on $\text{CdZr}_4\text{P}_6\text{O}_{24}$ [7] indicate R-3 as more suitable symmetry to account the ordered vacancies. In order to reveal the effect of vacancies and ionic radii of M on NZP frame, structural studies on $\text{Ca}_{1-x}\text{Ba}_x\text{Zr}_4\text{P}_6\text{O}_{24}$ compositions are carried out. The structural parameters, in particular, the location of anions and phosphorous atoms in such complex structures derived from neutron diffraction (ND) data are often superior compared to those derived from X-ray diffraction (XRD) data. Hence, combined powder ND and XRD studies are carried out to get accurate unit cell parameters and position coordinates. The results of these studies are presented in this manuscript.

2. Experimental

The nominal compositions of $\text{Ca}_{1-x}\text{Ba}_x\text{Zr}_4\text{P}_6\text{O}_{24}$ were prepared by solid state reactions of stoichiometric amounts of CaCO_3 , BaCO_3 , ZrO_2 and $(\text{NH}_4)_2\text{HPO}_4$. The initial mixture of the component reactants were heated at 300°C for about 5 h to decompose all the $(\text{NH}_4)_2\text{HPO}_4$ followed by rehomogenization and reheating at 900 and 1250°C for 24 h at each temperature with intermittent grinding. The colorless products obtained were characterized by powder XRD. The powder XRD data for structural analysis were recorded on a Philips x-pert pro diffractometer in the 2θ range of 10 – 100° , with step width of 0.02° , using $\text{CuK}\alpha$ radiation. The powder neutron diffraction data for $x = 0, 0.5$ and 1.0 compositions were recorded at Dhruva research reactor with neutron wavelength of 1.249 \AA . The structural studies were carried out by combined Rietveld refinement of the powder X-ray diffraction and neutron diffraction patterns using GSAS software package [8].

Table 1. Typical crystallographic parameters and residuals of the refinements for $\text{Ca}_{1-x}\text{Ba}_x\text{Zr}_4\text{P}_6\text{O}_{24}$.

$X =$	0	0.5	1.0
Space group	Trigonal R-3 (148)	Trigonal, R-3 (148)	Trigonal, R-3 (148)
Unit cell parameters	8.7741(4) Å	8.6903(4) Å	8.6399(3) Å
a, c and V	22.7035(12) Å 1513.7(2) Å ³	23.3861(11) Å 1529.5(2) Å ³	23.9747(9) Å 1549.9(2) Å ³
Formula unit	3	3	3
ρ (g/cc)	3.208	3.111	3.446
R_p, R_{wp} (XRD)	7.43, 9.99	8.78, 11.55	8.77, 11.4
R_p, R_{wp} (ND)	4.22, 5.40	4.12, 5.65	4.81, 6.36
χ^2	3.71	3.12	4.04
R_F^2 (XRD)	4.77	7.42	6.79
R_F^2 (ND)	5.67	6.30	6.75
Impurity phases	ZrP ₂ O ₇ (8 wt%)	ZrP ₂ O ₇ (5 wt%)	BaZrP ₂ O ₈ (3 wt%)

3. Results and discussion

The powder XRD patterns of the final products of nominal compositions $\text{Ca}_{1-x}\text{Ba}_x\text{Zr}_4\text{P}_6\text{O}_{24}$ are shown in figure 1. The XRD patterns of the two end members, namely, $\text{CaZr}_4\text{P}_6\text{O}_{24}$ and $\text{BaZr}_4\text{P}_6\text{O}_{24}$ were analysed by comparing with their earlier reported data. The phase purities of other compositions were ascertained by comparing the diffraction pattern with those of the end members. The unit cell parameters of all the compositions were determined by indexing the selected reflections of the powder XRD data and subsequently refining by the Rietveld method. The Rietveld refinement of $x = 0, 0.5$ and 1.0 were carried out by considering both XRD and neutron diffraction patterns with equal weight to both. The background of the powder XRD and ND data were modelled with fifth-order polynomial and linear interpolation of the selected refinable points. The observed Bragg peaks were modelled with pseudo-Voigt profile functions. It needs to be mentioned here that secondary phases like, BaZrP_2O_8 [9] and ZrP_2O_7 [10] were observed in some compositions. The diffraction data of these compositions were refined with multiphase contributions. The final refined unit cell parameters and the residuals of the refinements are given in table 1. The typical refined structural parameters for $x = 0.5$ are given in table 2. The final Rietveld refinement plots for ND and XRD data of $x = 0.5$ composition are shown in figures 2a and 2b respectively.

The analysis of the observed structural parameters shows the formation of an ideal solid solution between the two end members. This is in agreement with the iso-structural nature of the end members. The unit cell parameters show a gradual variation with the composition. It can be mentioned here that the a -axes of the rhombohedral lattice decreases with increase in Ba^{2+} concentration despite the higher ionic radius of Ba^{2+} than Ca^{2+} . However, the c -axis gradually increases with the increase in Ba^{2+} concentrations. The increase in unit cell volume with the increase in the Ba^{2+} concentration is in accordance with the larger ionic size of Ba^{2+} . The variation of unit cell volume with composition can be represented as V (Å³) = 1514.4(9) + 0.029(4) × X + 0.0006(4) × X^2 , where $X = \%$ of Ba.

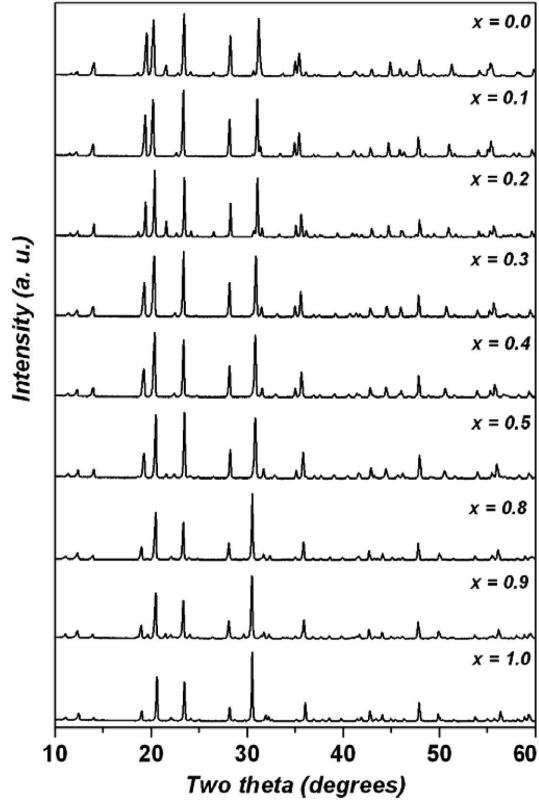


Figure 1. Powder XRD patterns of $\text{Ca}_{1-x}\text{Ba}_x\text{Zr}_4\text{P}_6\text{O}_{24}$.

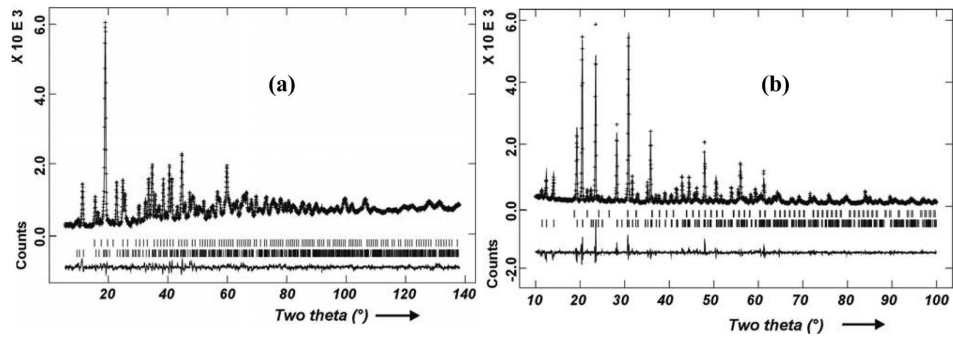


Figure 2. The typical Rietveld refinement plots for $\text{Ca}_{0.5}\text{Ba}_{0.5}\text{Zr}_4\text{P}_6\text{O}_{24}$. (a) ND and (b) XRD. Vertical marks between diffraction pattern and difference plot indicate Bragg positions for ZrP_2O_7 (upper) and $\text{Ca}_{0.5}\text{Ba}_{0.5}\text{Zr}_4\text{P}_6\text{O}_{24}$ (lower).

Table 2. Refined position coordinates and thermal parameters (\AA^2) for $Ca_{0.5}Ba_{0.5}Zr_4P_6O_{24}$.

Atom	x	y	z	U_{11}	U_{22}	U_{33}	U_{12}	U_{13}	U_{23}
Ca	0	0	0	0.028(2)	0.028(2)	0.032(4)	0.014(1)	0	0
Ba	0	0	0	0.028(2)	0.028(2)	0.032(4)	0.014(1)	0	0
Zr1	0	0	0.1501(1)	0.005(1)	0.005(1)	0.035(3)	0.003(1)	0	0
Zr2	0	0	0.6446(1)	0.006(1)	0.006(1)	0.040(3)	0.003(1)	0	0
P	0.29026(5)	0.0032(8)	0.2508(4)	0.007(3)	0.005(2)	0.041(3)	0.004(3)	0.000(4)	0.007(2)
O1	0.18757(8)	-0.0081(8)	0.1992(3)	0.013(4)	0.035(4)	0.033(5)	0.015(3)	0.003(3)	0.025(3)
O2	0.0628(8)	-0.1594(8)	0.6961(3)	0.020(4)	0.014(4)	0.030(5)	0.002(3)	0.030(4)	0.002(3)
O3	0.1866(8)	0.1852(8)	0.0912(3)	0.022(4)	0.012(4)	0.021(5)	-0.000(3)	0.011(4)	0.022(3)
O4	-0.1623(8)	-0.2095(9)	0.5933(3)	0.007(4)	0.015(4)	0.056(6)	0.002(3)	-0.007(3)	-0.024(3)

Ca : Ba = 3a (0,0,0) occ. 0.51(1);0.49(1); Zr1 and Zr2: 6c; (0, 0, z); P and O's: 36i: (x, y, z)
 ($a = 8.6903(4) \text{\AA}$, $c = 23.3861(11) \text{\AA}$ and $V = 1529.54(16) \text{\AA}^3$)
 (ZrP₂O₇; $a = 8.2729(1) \text{\AA}$, $V = 566.20(2) \text{\AA}^3$, space group: Pa-3).

The refined position coordinates show no appreciable change in the PO₄ tetrahedra or ZrO₆ octahedra. The observed P–O bonds in CaZr₄P₆O₂₄ and BaZr₄P₆O₂₄ are in the range of 1.46–1.57 Å. Similarly, the Zr–O bonds for Zr1 and Zr2 in both BaZr₄P₆O₂₄ and CaZr₄P₆O₂₄ are in the range of 2.06–2.13 and 2.02–2.09 Å, respectively. However, there is a significant change in the M–O bond by changing the M ion from Ca²⁺ to Ba²⁺. The typical M–O bonds in BaZr₄P₆O₂₄ and CaZr₄P₆O₂₄ are 2.795 and 2.475 Å, respectively, which are in accordance with the ionic radii of Ba²⁺ ($r = 1.35$ Å) and Ca²⁺ ($r = 1.00$ Å). The M ions of MZr₄P₆O₂₄ form distorted MO₆ octahedra with more elongation along the *c*-axis. The elongation of MO₆ increases with the increase in Ba²⁺ concentration. These elongations are reflected by the increase in *c*-axes parameters with increase in Ba²⁺ concentration.

4. Conclusions

In conclusion we observe that Ba²⁺ and Ca²⁺ ions of the mixed Ca_{1-x}Ba_xZr₄P₆O₂₄ composition are statistically occupied in the 3a site of the R-3 lattice. All the studied compositions crystallize in rhombohedral (R-3) lattice. No indication of the R-3c symmetry is observed in any composition. The variation of M–O, M = Ba or Ca, and the elongation parameter of the MO₆ octahedra are reflected in the variation of the unit cell parameters with composition.

References

- [1] S Y Limaye, D K Agrawal and R Roy, *J. Mater. Sci.* **26**, 93 (1991)
- [2] G Harshe and D K Agrawal, *J. Am. Ceram. Soc.* **77**, 1965 (1994)
- [3] L Hagman and P Kierkegaard, *Acta. Chem. Scand.* **22**, 1822 (1968)
- [4] P S Tantri, K Geetha, A M Umarji and S K Ramesha, *Bull. Mater. Sci.* **23**, 491 (2000)
- [5] E Brevel and D K Agrawal, *Br. Ceram. Soc.* **94**, 27 (1995)
- [6] D A Woodcock, P Lightfoot and C Ritter, *Chem. Comm.* **107**, (1998)
- [7] R Brochu, M Louer, M Alami, M Alqaraoui and D Louer, *Mater. Res. Bull.* **32**, 113 (1997)
- [8] A C Larson and R B van Dreele, GSAS: General Structure Analysis System, Los Alamos National Laboratory, Report LAUR 86-748, 2000
- [9] K Fukuda, A Moriyama and T Iwata, *J. Solid State Chem.* **178**, 2144 (2005)
- [10] M Chaunac, *Bull. Soc. Chim. France* **1971**, 424 (1971)